Localization of Low-Frequency Oscillations in Single-Walled Carbon Nanotubes

V. V. Smirnov,* D. S. Shepelev, and L. I. Manevitch
Institute of Chemical Physics, Russian Academy of Sciences, 4 Kosygin Street, 119991 Moscow, Russia
(Received 30 September 2013; revised manuscript received 25 November 2013; published 23 September 2014)

In the framework of the continuum shell theory, we analytically predict a new phenomenon: the weak localization of optical low-frequency oscillations in carbon nanotubes. We clarify the origin of the localization by means of the concept of the limiting phase trajectory and confirm the obtained analytical results by molecular dynamics simulations of simply supported carbon nanotubes. The performed analysis contributes to the new universal approach to the treatment of nonstationary resonant processes.

DOI: 10.1103/PhysRevLett.113.135502 PACS numbers: 62.25.-g, 05.45.-a, 63.20.D-, 63.22.Gh

Advances in nanoscience open the possibilities for the experimental realization of some nonlinear dynamical phenomena earlier considered only in model systems [1–4]. Examination of carbon nanotubes (CNTs), graphene nanoribbons, and nanowires allows us to observe these phenomena [5–7] as well as to develop new supersmall and ultrafast devices [8–11]. The nano-objects do not contain dislocations and plasticity is absent. Therefore, one should expect that the results of molecular dynamics (MD) simulations (with force fields obtained in quantum chemical calculations) will conform with the experiment.

In linear systems, the processes of heat or energy transfer are traditionally associated with phonons as normal modes of the respective dynamical systems [12,13]. In nonlinear systems, the main competitors for the energy transfer are localized excitations—solitons and breathers [14,15]. To minimize the spatial spreading of a phonon packet, it is necessary that the normal modes in the packet should have close frequencies. However, in the presence of nonlinearity, the resonant interactions between these modes will take place. Below we will show that the effect of the nonlinear resonant phonon interactions in such a classical system as a carbon nanotube with a finite length results in nontrivial consequences such as the low-frequency energy localization and/or energy exchange. The energy localization corresponds to a breather in an infinite system, while the energy exchange does not have a counterpart in an infinite system.

Recently, we proposed [16] an analogy between the low-frequency shell-like vibrations of a single-walled CNT and the nonlinear dynamics of a one-dimensional oscillator chain (see, also, the Supplemental Material [17]). It was also shown that intermodal interaction under conditions of $1:1$ resonance can lead (under some specific conditions) to intensive energy exchange between different parts of the system or to the spatial localization of the energy [18–20]. However, the realistic CNT model turns out to be much more complicated.

In the CNT spectrum, there are two optical-type branches that are interesting from the viewpoint of mode interaction. The first branch is the well-known radial breathing mode (RBM) (azimuthal wave number $n = 0$) corresponding to uniform radial expansion compression. The second mode ($n = 2$) describes deviation of the CNT cross section from a circuit (circumferential flexure mode, CFM) [21,22]. In spite of possible nonlinear coupling of vibrations belonging to different oscillation branches [23], the interaction between two low-frequency CF modes can be predominant for a certain set of the CNT's parameters due to the proximity of the frequencies.

Let us consider oscillations corresponding to the CFM branch. The displacement field of carbon atoms is shown in Fig. 1(a). It is reasonable to assume that on this branch the ring and shear deformations are small, and, therefore, the shape of the CNT transversal cross section changes without an elongation of the contour line. In such a case, the energies of the tangential and longitudinal deformations can be neglected and the corresponding components of the displacements can be expressed via the radial component. Some details of the analysis of the CNT vibrations are presented in the Supplemental Material [17].

As we already mentioned, the spectrum branch of the CFM is an optical-type branch, and the value of the gap is determined by the own flexural rigidity of the CNT transversal cross section. Therefore, regardless of the type of boundary conditions, there is a crowding of the

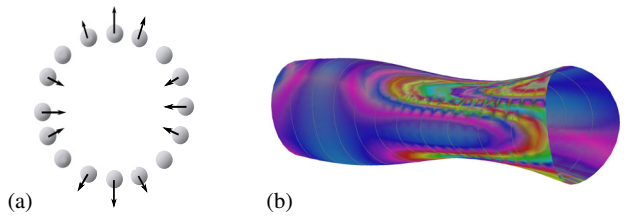

FIG. 1 (color online). (a) Displacements of carbon atoms in CFM. The arrows show directions and relative values of the atomic displacements. (b) Energy distribution along the CNT when a certain combination [ψ_2, see Eq. (4)] of the first two modes on the CFM branch is excited; dark blue zone (low energy), red zone (high energy).

eigenvalues near the low-frequency (long-wave) boundary. We estimated that if the aspect ratio of the CNT exceeds 15, the distance between the frequencies of the first and the second modes is small enough, and its value is approximately twice less than the distance between the second and the third modes. This allows one to restrict the analysis to the two-mode approximation.

One can show that the nonlinear interaction of the low-frequency normal modes in the framework of two-mode approximation is described by a system of equations, the structure of which is general for various systems with discrete spectrum—from a pair of weakly bounded anharmonic oscillators to nonlinear lattices of a finite size. The derivation procedure of these equations is described in Ref. [18]. For the low-frequency CNT dynamics, these equations can be written as follows:

$$i\frac{\partial\chi_1}{\partial\tau} + 2a_1|\chi_1|^2\chi_1 + a_3|\chi_2|^2\chi_1 + 2a_4\chi_2^2\chi_1^* = 0,$$
$$i\frac{\partial\chi_2}{\partial\tau} + \omega_1\chi_2 + a_3|\chi_2|^2\chi_1 + 2a_2|\chi_2|^2\chi_2 + 2a_4\chi_1^2\chi_2^* = 0, \quad (1)$$

where χ_1 and χ_2 are complex amplitudes of the modes in the leading order, and the asterisk denotes complex conjugation.

The coefficients a_j are determined by geometry of the CNT and by its Poisson ratio (see the Supplemental Material [17]), and ω_1 is the natural frequency of the first mode. In Eqs. (1), the variable τ is a slow time ($\tau = \varepsilon^2 t$), and the small parameter ε is determined by the relative difference between the modal frequencies: $\varepsilon = \sqrt{(\omega_2 - \omega_1)/\omega_1}$. It is very important that the complex amplitudes χ_j depend only on the slow time. Equations (1) are characteristic for resonance interaction of two objects. One can show that the behavior of the system depends drastically on the relation between parameters a_1, a_2, a_3, and a_4. The nonlinear terms with coefficients a_1, a_2, and a_3 are responsible for frequency shifts, while the last term with factor a_4 provides nonlinear interaction between the modes under consideration.

Equations (1) correspond to the Hamiltonian

$$H = \omega_1|\chi_2|^2 + a_1|\chi_1|^4 + a_2|\chi_2|^4 + a_3|\chi_1|^2|\chi_2|^2 + a_4(\chi_1^2\chi_2^{*2} + \chi_1^{*2}\chi_2^2) \quad (2)$$

of quite a general form describing a nonlinear system of two weakly coupled components, accounting for the nonlinear interaction between the components up to fourth order.

Besides the obvious energy integral (2), Eqs. (1) possess another integral (occupation number integral in quantum-mechanical terminology):

$$X = |\chi_1|^2 + |\chi_2|^2. \quad (3)$$

This parameter characterizes the total excitation of the system. The analysis of Eqs. (1) shows that the normal modes under resonance conditions being strongly interactive become inadequate for the description of the nonstationary behavior. This description should use weakly interacting objects. As it turns out, in the system under consideration, this role can be played by such combinations of the nonlinear normal modes (NNMs) which represent excitations of different parts of the CNT. Namely,

$$\psi_1 = \frac{1}{\sqrt{2}}(\chi_1 + \chi_2); \qquad \psi_2 = \frac{1}{\sqrt{2}}(\chi_1 - \chi_2). \quad (4)$$

Indeed, considering the distribution of energy along the nanotube, one can see that these linear combinations of normal modes provide predominant energy concentration in the left or right part of the CNT, while the other part of the CNT has much lower energy density [Fig. 1(b)]. Because of the small difference between the frequencies of the modes χ_1 and χ_2, the two parts of the CNT demonstrate some coherent behavior similar to beating in the system of two weakly coupled oscillators. Therefore, we can consider these regions as new large-scale elementary units of the system, "effective particles" introduced for discrete nonlinear lattices in Ref. [18].

The existence of the integral of motion (3) allows us to reduce the phase space of the system up to two dimensions. Now we can introduce real variables *a priori* conserving the integral (3):

$$\psi_1 = \sqrt{X}\cos(\theta)e^{-i\delta/2}; \qquad \psi_2 = \sqrt{X}\sin(\theta)e^{i\delta/2}. \quad (5)$$

In the reduced phase space, the first variable (θ) characterizes the relative amplitudes of the effective particles ψ_1 and ψ_2, and the second one (δ) is the phase shift between them.

Now we can rewrite Hamiltonian (2) in terms of "angle" variables θ and δ:

$$H = \frac{X}{16}\{8\omega_1(1 - \cos\delta\sin 2\theta) + X[4a_1(\cos\delta\sin 2\theta + 1)^2 + 4a_2(\cos\delta\sin 2\theta - 1)^2 + a_3(2\cos^2\delta\cos 4\theta - \cos 2\delta + 3) + 2a_4(2\cos^2\delta - (\cos 2\delta - 3)\cos 4\theta)]\}. \quad (6)$$

A typical phase portrait of a system with Hamiltonian (6) for small excitation level X is shown in Fig. 2(a). Two steady states with $\theta = \pi/4$ and $\delta = 0$ and $\delta = \pi$ correspond to normal modes χ_1 and χ_2. The trajectories surrounding these stationary points describe the dynamics of effective particles; i.e., they show the evolution of variables ψ_1 and ψ_2. The values $\theta = 0$ and $\theta = \pi/2$ correspond to energy concentration on one of the effective particles. When these

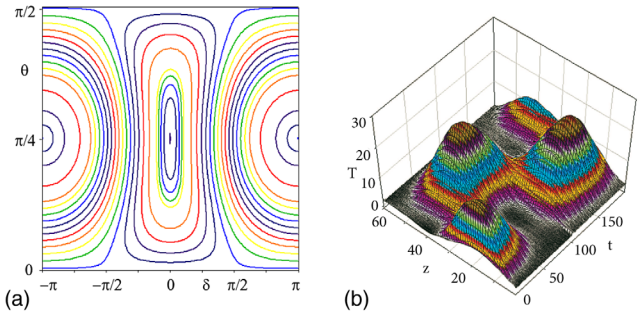

FIG. 2 (color online). (a) Phase portrait of the system (6) with a low level of excitation $X = 0.05$. (b) The energy distribution along the CNT with aspect ratio $\lambda = 32$ in the MD simulation of the LPT. The level of excitation corresponds to the phase portrait in (a). Energy is measured in kelvin and time—in picoseconds.

values are reached, the energy distribution along the CNT is the most nonuniform. These states belong to the phase trajectory maximally distant from the stationary points χ_1 and χ_2. Consequently, the motion along the trajectory is accompanied with the energy transfer from one part of the CNT to another one. Such a trajectory has been termed as the limiting phase trajectory (LPT) because it encircles the domain of attraction of the stationary points at maximal distance [18–20]. The motion along a LPT is similar to beats in a system of two oscillators [24], and here the parts of the CNT play the role of effective particles. This process is illustrated in Fig. 2(b), where the energy distribution along the CNT during MD simulation of the zigzag CNT vibrations is shown. We used the following parameters of the CNT: length $L = 25.4$ nm, radius $R = 0.79$ nm (the aspect ratio $\lambda = 32$), and the boundary conditions corresponded to the simply supported nanotube. (Some details of the MD simulation are described in the Supplemental Material [17].) The initial temperature of the nanotube was 1.0 K, and the initial velocity field corresponded to the linear combination of two low-frequency modes. To show the energy in Fig. 2(b), the considered CNT was separated into 60 "elementary rings," and each of them contained 40 carbon atoms.

What occurs when the parameter X grows? Figures 3(a) and 3(b) show two phase portraits corresponding to larger values of X. We see that the topology of these portraits essentially differs from that in Fig. 2(a). Namely, besides the stationary points χ_1 and χ_2, an additional pair of steady states arises as a result of instability of the lowest-frequency normal mode at the excitation level

$$X = X_u = \omega_1/(2a_1 - a_3 - 2a_4). \tag{7}$$

The new steady states, as long as they are close to the "parent" normal mode, represent only nonlinear normal modes with relatively small energy excess in one part of the CNT. Most importantly, the possibility of the complete energy exchange between the CNT parts is preserved. With

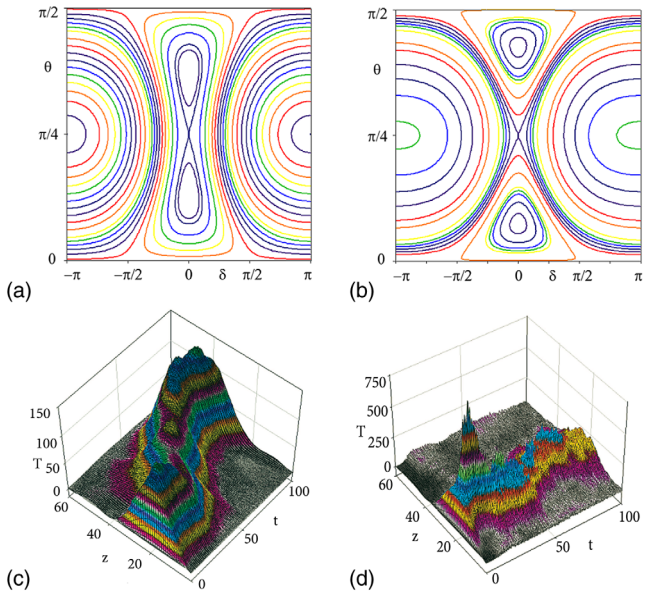

FIG. 3 (color online). Phase portraits (a),(b) of the system (6) and energy distributions along the CNT in the MD simulations of the LPTs (c),(d) at large excitation levels X for CNTs with aspect ratio $\lambda = 32$. Left panel: $X = 0.15$. Right panel: $X = 0.25$. Energy is measured in kelvin and time—in picoseconds.

the growth of the parameter X, the new stationary states depart further from the original normal mode, and, consequently, the separatrix loop expands. At the point

$$X = X_{\text{loc}} = 2\omega_1/(3a_1 - a_2 - a_3 - 2a_4), \tag{8}$$

the separatrix merges with the LPT. This threshold signifies the complete energy localization, since any path starting at the upper half of the phase plane cannot reach the bottom half and vice versa.

The instability threshold for the CNT with the considered aspect ratio is $X_u = 0.08$, and the localization threshold is $X_{\text{loc}} = 0.17$. The energy distributions along the z axis of the CNT obtained in the MD simulation of the LPTs are shown in Figs. 3(c) and 3(d). One can see that near the localization threshold, the beating shown in Fig. 2(b) transforms into a long-time flow of the energy from one part of the CNT to another [Fig. 3(c)]. Figure 3(d) shows the energy distribution along the CNT at the excitation level significantly exceeding the localization threshold. One can see that no energy flow along the CNT occurs. Although the energy profile during the simulation differs significantly from the initial one, its location preserves.

We saw that the instability of the band-edge optical mode of the CNT vibrations is a preliminary condition of energy localization in some part of the CNT. However, the energy capture in one of the CNT parts can be achieved if the excitation level exceeds the specified threshold corresponding to merging of two trajectories—the LPT and the separatrix. Simultaneously, between the two LPTs, a set of

trajectories passing all the values of the phase shift δ is created. The energy capture does not mean the generation of strongly localized excitations whose formation requires participation of additional modes of the spectrum. The two-mode approximation gives the "weak" energy localization, becoming strong enough if the excitation level grows and additional modes get into the resonant conditions.

An important point is that the phenomenon of energy localization considered above is a common peculiarity of the systems possessing optical-type branches of a spectrum. In particular, one can expect that the RBM can also manifest the energy capture in effective particles. The only difference is in the type of localization. Because we assume "hard" nonlinearity in the RBM branch, we should expect a "dark-type" localized solution in contrast with the CFM branch, where nonlinearity is "soft." We hope that these processes can be observed experimentally.

Finally, we should note that the discussed nonlinear dynamical phenomena are peculiar to systems with a nonequidistant discrete spectrum. Therefore, the analysis based on the LPT concept is appropriate for the wide class of nano-objects. It is also important that the dynamical behavior considered above can exist at either the low- or high-frequency side of the spectrum. These nonlinear processes may substantially affect thermal and electrical transport in nanotubes, nanoribbons, and nanowires.

The work was supported by the Department of Chemistry and Material Science of Russian Academy of Sciences (Program No. 1), Russian Academy of Sciences, and the Russian Foundation for Basic Research (Grant No. 08-03-00420a).

*vvs@polymer.chph.ras.ru

[1] E. Fermi, J. Pasta, and S. Ulam, in *Collected Papers of Enrico Fermi*, edited by E. Segre (University of Chicago Press, Chicago, 1965), Vol. 2, p. 978.
[2] M. Toda, *Theory of Nonlinear Lattices*, 2nd ed., Springer Series in Solid-State Sciences Vol. 20 (Springer, Berlin, 1989), p. 225.
[3] O. M. Braun and Y. S. Kivshar, *The Frenkel-Kontorova Model. Concepts, Methods, and Applications*, Theoretical and Mathematical Physics Vol. XVIII (Springer, New York, 2004), p. 475.
[4] A. C. Scott, *Nonlinear Science: Emergence and Dynamics of Coherent Structures*, 2nd ed. (Oxford University Press, Oxford, 2003), p. 480.
[5] N. Mingo and D. A. Broido, Nano Lett. **5**, 1221 (2005).
[6] B. Li, J. Wang, L. Wang, and G. Zhang, Chaos **15**, 015121 (2005).
[7] Y. Zhong, Y. Zhang, J. Wang, and H. Zhao, Phys. Rev. E **85**, 060102(R) (2012).
[8] M. P. Anantram and F. Lonard, Rep. Prog. Phys. **69**, 507 (2006).
[9] Ch. Ke and H. D. Espinosa, *Handbook of Theoretical and Computational Nanotechnology*, edited by W. M. Riethand (American Scientific Publishers, New York, 2005), Vol. 1, p. 1.
[10] V. Sazonova, Y. Yaish, H. Stnel, D. Roundy, T. A. Arias, and P. L. McEuen, Nature (London) **431**, 284 (2004).
[11] H. B. Peng, C. W. Chang, S. Aloni, T. D. Yuzvinsky, and A. Zettl, Phys. Rev. Lett. **97**, 087203 (2006).
[12] S. Lepri, R. Livi, and A. Politi, Phys. Rep. **377**, 1 (2003).
[13] X. Zhang, M. Hu, and D. Poulikakos, Nano Lett. **12**, 3410 (2012).
[14] N. Li, B. Li, and S. Flach, Phys. Rev. Lett. **105**, 054102 (2010).
[15] D. Cai, A. R. Bishop, and N. Grønbech-Jensen, Phys. Rev. E **52**, R5784 (1995).
[16] V. V.Smirnov, D. S. Shepelev, and L. I. Manevitch, Nanosys. Phys. Chem. Math. **2**, 102 (2011).
[17] See Supplemental Material at http://link.aps.org/supplemental/10.1103/PhysRevLett.113.135502 for the details of the analysis of the nonlinear vibrational modes, the analogy with the nonlinear chains, and the description of MD simulation.
[18] L. I. Manevitch and V. V. Smirnov, Phys. Rev. E **82**, 036602 (2010).
[19] L. I. Manevitch and V. V. Smirnov, Dokl. Phys. **55**, 324 (2010).
[20] V. V. Smirnov and L. I. Manevitch, Acoust. Phys. **57**, 271 (2011).
[21] A. M. Rao, E. Richter, S. Bandow, B. Chase, P. C. Eklund, K. A. Williams, S. Fang, K. R. Subbaswamy, M. Menon, A. Thess, R. E. Smalley, G. Dresselhaus, and M. S. Dresselhaus, Science **275**, 187 (1997).
[22] M. S. Dresselhaus and P. C. Eklund, Adv. Phys. **49**, 705 (2000).
[23] P. A. Greaney, G. Lani, G. Cicero, and J. C. Grossman, Nano Lett. **9**, 3699 (2009).
[24] L. Manevitch, Arch. Appl. Mech. **77**, 301 (2007).